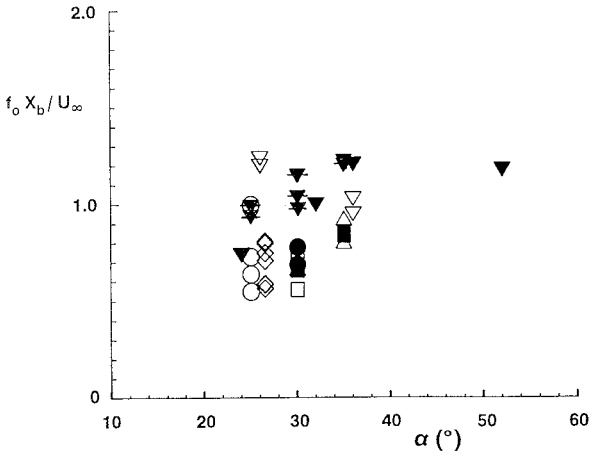

Fig. 3 Dimensionless frequency $f_0 x_b / U$ of peak of spectrum of surface pressure fluctuation as a function of angle-of-attack α; distance x_b is from onset of vortex breakdown to location of pressure transducer.

trend, no doubt, due to the complexity of these configurations, the extreme values of frequency $f_0 x/U_0$ approximately correspond to the extreme values for the simple delta wing–fin configurations Δ_F. The major share of the data lie in the range $1.0 \leq f_0 x/U_0 \leq 3.0$. The fact that these dimensionless frequencies lie within a definable band of dimensionless frequencies $f_0 x/U_\infty$ suggests that the same principal mechanism is responsible for their generation. The occurrence of large-scale instabilities in the wake type bubble, immediately following the onset of vortex breakdown, appears to be the principal excitation mechanism over a wide range of Reynolds and Mach numbers, and it appears that scaling on the basis of x, the distance from the origin of the vortex, is a reasonable approximation for determining the order of the predominant frequency.

For certain experiments listed in Table 1, it is possible to deduce the location of vortex breakdown and thereby determine the distance x_b from the onset of breakdown to the location of the pressure tap on the fin. The plot of Fig. 3 shows that the data normalized on this basis lie in the range $0.5 \leq f x_b/U_0 \leq 1.3$. Recasting $f x_b/U_0$ as $x_b/(U_0/f)$, the distance, x_b appears to be of the same order as an equivalent freestream wavelength $\lambda_0 = U_0/f$. Of course, the wavelength λ of the instability within the vortex increases substantially in the streamwise direction after the onset of breakdown. Further insight into the flow structure is required to relate this wake instability to the data correlation of Fig. 3.

Acknowledgments

The authors are pleased to acknowledge support of the Air Force Office of Scientific Research through Grants AFOSR-91-0055, F49620-93-1-0075, and F49620-94-1-0038.

References

[1]Bean, D. E., and Wood, N., "An Experimental Investigation of Fin Buffeting and Suppression," AIAA Paper 93-0054, Jan. 1993.

[2]Washburn, A. E., Jenkins, L. M., and Ferman, M. A., "Experimental Investigation of Vortex-Fin Interaction," AIAA Paper 93-0050, Jan. 1993.

[3]Wolfe, S., and Rockwell, D., "Buffeting of a Leading-Edge by a Streamwise Vortex: Instantaneous Flow Structure and Surface Pressure Loading," *Journal of Fluids and Structures* (to be published).

[4]Canbazoglu, S., Lin, J.-C., Wolfe, S., and Rockwell, D., "Buffeting of Fin: Distortion of Incident Vortex," *AIAA Journal* (to be published).

[5]Triplett, W. E., "Pressure Measurements on Twin Vertical Tails in Buffeting Flow," *Journal of Aircraft*, Vol. 20, No. 11, 1983, pp. 920–925.

[6]Wentz, W. H., Jr., "Vortex-Fin Interaction on a Fighter Aircraft," *Proceedings of the AIAA 5th Applied Aerodynamics Conference* (Monterey, CA), AIAA, Washington, DC, 1987, pp. 392–399 (AIAA Paper 87-4909).

[7]Ferman, N. A., Patel, S. R., Zimmerman, N. H., and Gerstenkorn, G., "A Unified Approach to Buffet Response of Fighter Aircraft Empennage," *AGARD/NATO 70th Structures and Materials Meeting*, Sorento, Italy, 1990, pp. 2-1–2-15.

[8]Shah, G. H., "Wind-Tunnel Investigation of Aerodynamic and Tail Buffet Characteristics of Leading-Edge Extension Modifications to the F/A-18," 2889, AIAA Paper 91-2889, Aug. 1991.

[9]Lee, B. H. K., and Tang, F. C., "Buffet Load Measurements on an F/A-18 Vertical Fin at High-Angle-of-Attack," AIAA Paper 92-2127, 1992.

[10]Martin, C. A., and Thompson, D. H., "Scale Model Measurements on Fin Buffet Due to Vortex Bursting on F/A-18," AGARD/CP 497.

[11]Lee, B. H. K., Brown, D., Tang, F. C., and Plosenski, M., "Flow Field in the Vicinity of an F/A-18 Vertical Fin at High-Angle-of-Attack," *Journal of Aircraft*, Vol. 30, No. 1, 1993, pp. 69–74.

[12]Liebovich, S., "Vortex Stability and Breakdown: Survey and Extension," *AIAA Journal*, Vol. 22, No. 9, 1984, pp. 1192–1206.

[13]Brown, G. L., and Lopez, J. M., "Axisymmetric Vortex Breakdown. Pt. 2: Physical Mechanism," *Journal of Fluid Mechanics*, Vol. 221, 1990, pp. 553–576.

[14]Garg, A. K., and Leibovich, S., "Spectral Characteristics of Vortex Breakdown Flow Fields," *Physics of Fluids*, Vol. 22, No. 11, 1979, pp. 2053–2064.

[15]Roos, F. W., and Kegelman, J. T., "Recent Explorations of Leading-Edge Vortex Flow Fields," NASA High-Angle-of-Attack Technology Conf., NASA Langley Research Center, Hampton, VA, Oct.–Nov. 1990.

[16]Gursul, I., "Unsteady Flow Phenomena Over Delta Wings at High Angle of Attack," *AIAA Journal*, Vol. 32, No. 2, 1994, pp. 225–231.

[17]Towfighi, J., and Rockwell, D., "Instantaneous Structure of Vortex Breakdown on a Pitching Delta Wing," *AIAA Journal*, Vol. 31, No. 7, 1993, pp. 1160–1162.

[18]Lin, J.-C., and Rockwell, D., "Transient Structure of Vortex Breakdown on a Delta Wing at High Angle-of-Attack," *AIAA Journal*, Vol. 33, No. 1, 1995, pp. 6–12.

[19]Lee, B. H. K., and Brown, D., "Wind Tunnel Studies of F/A 18 Tail Buffet," *Journal of Aircraft*, Vol. 29, No. 1, 1992, pp. 146–152.

Flow Visualization Using Natural Condensation of Water Vapor

Michael Brendel*
Centerville, Ohio 45459

I. Introduction

RECENT interest in transonic axial compressor rotors has driven a need for the development of a flow visualization technique to assess characteristic flow structures that impact rotor performance. Losses associated with blade passage shock waves and/or blade tip vortex–shock interactions are not well understood. Numerous experimental studies, generally involving the measurement of casing surface pressures (steady) or wake pressure distributions, offer little insight into detailed blade passage flow structure. It is clear that measurement of the internal flow structure requires a nonintrusive technique since the disturbance introduced by conventional pressure and/or thermal sensors will alter the natural flow. Furthermore, the adaptation of intrusive sensors is operating turbomachinery presents a formidable engineering challenge. The purpose of the present Note is to describe a planar imaging technique which makes use of condensing water vapor. Implementation of the technique is straightforward in steady flow applications and, thus, offers a cost effective means to visualize high-speed flows. The work presented here was part of pilot study to demonstrate a flow visualization technique which could be adapted to an operating compressor rotor environment.

The use of Mie scattering in flow visualization is commonplace at low speeds.[1] Applications involving higher speeds are less well known but have been demonstrated. Goddard et al.[2] appear to have been the first to successfully introduce smokelines, formed by vaporizing an oil into a transonic flow. Images were recorded on photographic film simultaneously with schlieren images. McGregor[3] considered condensation of water vapor as a means to visualize flows over transonic delta wings. The formation of condensed vapor in those experiments was a result of low stagnation pressures and temperatures used in a closed-loop wind tunnel. Flow pressures and temperatures are not always conducive to condensation except

Received Nov. 30, 1994; revision received Jan. 16, 1995; accepted for publication Jan. 25, 1995.

*Engineering Consultant. Senior Member AIAA.

in isolated regions of depressed temperatures and pressures, such as in vortical flows. In addition to wind-tunnel applications, condensed water vapor has been considered in flight experiments.[4]

The present work involves the use of naturally occurring condensed water vapor as flow tracer in a blown-down wind tunnel with a laser light sheet as the illumination source. Images are obtained with a digital camera and then recorded on a microcomputer for processing and interpretation. This represents an advance over prior attempts which relied upon conventional photographic methods. The focus of this study is to determine the suitability of the technique to resolve flow features in a transonic flow. Digital flow visualizations of the flow about simple models placed at the exit of a converging–diverging (C–D) nozzle are presented.

II. Experimental Apparatus

All testing was conducted in the University of Dayton supersonic blowdown facility. Ambient air was compressed and then accumulated in a 1.45-m^3 (51-ft^3) bottle. A Bourdon-tube pressure gauge and *J* type thermocouple were used to monitor total pressure and total temperature, respectively. The bottle was connected to a 0.034-m^3 (1.2-ft^3) cast iron stagnation chamber through a 50-mm- (2-in.-) diam cast iron pipe containing a quick-action ball valve. A specially designed nozzle fixture was attached to the stagnation chamber with a short section cast iron pipe. This fixture allowed rapid changing of the converging–diverging nozzle used in the study. Nozzles having design Mach numbers of 1.5 and 2.0 were fabricated using the method of characteristics.

Illumination was provided by a Spectra-Physics Model 127 helium–neon laser ($\lambda = 614$ nm) having a rated output of 35 mW. Small first-surface mirrors were used to horizontally steer the laser beam to a position just below the nozzle exit. Here, a first-surface mirror inclined at 45 deg deflected the beam normal to the longitudinal axis of the nozzle. A small glass cylinder 4 mm (0.16 in.) in diameter was used to refract the laser beam into a sheet of light.

Flow visualization images were recorded with a Photometrics Ltd. STAR I digital camera. The system features a 576 × 384 pixel Thompson TH7883 scientific-grade charge-coupled device (CCD) for image acquisition through a 50-mm Nikon AF lens. Images were digitized directly from the CCD by a 12-bit analog-to-digital converter and then downloaded to a microcomputer through a General Purpose Interface Bus (GPIB) for processing and interpretation. The CCD was thermoelectrically cooled to −45°C (−50°F) to minimize effects of thermal agitation. Light sensitivity several orders of magnitude better than conventional video-based technology was achieved.

III. Results

The images presented here are representative of the large collection obtained in the study. The shock structures observed in these images were repeatable. Common to all of the images are the appearance of light striations caused by imperfections in the cylindrical lens used to spread the laser beam into the light sheet. Since the camera position relative to the plane of the image remained nearly constant for each test, the field of view measures approximately 96 × 64 mm (3.8 × 2.5 in.). This translates to a resolution of about 6 pixels/mm. This level of resolution allows one to infer shock angles within several degrees.

The flow over a 3-mm- (0.12-in.-) diam cylinder is shown in Fig. 1. The cylinder was placed just at the exit of the Mach 2.0 nozzle and is somewhat obscured by reflected light in the image. The flow

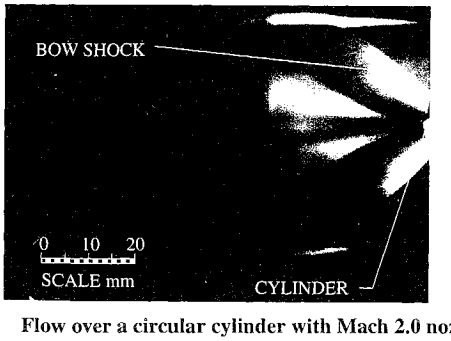

Fig. 1 Flow over a circular cylinder with Mach 2.0 nozzle.

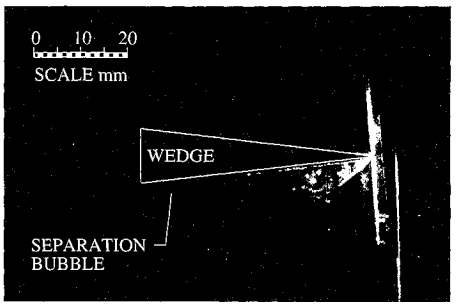

Fig. 2 Flow over a 5.8-deg half-angle wedge with Mach 2.0 nozzle.

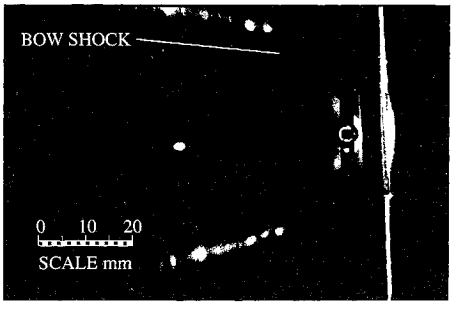

Fig. 3 Flow over a circular cylinder with Mach 1.5 nozzle.

is slightly underexpanded as evidenced by the divergence of the shear layers on both sides of the nozzle. The bow shock and wake recompression shock are clearly visible. Weak Mach waves can be seen emanating from the corners of the nozzle in the original image. Other Mach waves can be seen forward of the bow shock. Assuming a locally two-dimensional flow, the angle of these Mach lines indicates a flow Mach number of about 1.8. This interpretation appears reasonable but should not be taken too literally since the expansion zone just downstream of the nozzle is three dimensional. The asymptotic behavior of the bow shock is not a good indicator of Mach number in this case because of the interaction with reflected expansion and compression waves outside the nozzle.

Figure 2 shows the flow over a single wedge having a half-angle of 5.8 deg. The wedge was placed 5.2 mm (0.20 in.) from the exit of the Mach 2.0 nozzle. The laser light sheet, originating from below, was reflected back onto the upper surface of the wedge by a mirror above and out of view of the image. The oblique shock on the upper surface of the wedge appears to be straight and swept back at about 41 deg. Assuming a Mach number of 1.8 and a wedge half-angle of 5.8 deg, oblique shock theory predicts a shock angle of 39 deg. This agreement is quite good considering the uncertainty in the flow direction relative to the wedge angle. The bow shock formed on the lower surface is curved. It is likely that some ice accretion has taken place on this surface and that a small "bump" of glaze ice has altered the shock pattern. In addition, the lower portion of the leading edge had a slight bevel, whereas the upper surface had a sharp leading edge. Another notable feature of this flow visualization is the appearance of shock induced separation near the rear of the wedge. Compression waves emanating from the shear layer have coalesced to form a shock wave which then impinges on the lower surface of the wedge. The incident shock is at an angle of about 20 deg relative to the horizontal whereas the induced shock is at about 45 deg to the horizontal. This phenomenon is more clearly seen in the Mach 1.5 images discussed next. The height of the separation bubble in this image is about 0.8 mm (0.03 in.).

The bow shock ahead of a 3-mm- (0.12-in.-) diam cylinder using the Mach 1.5 nozzle is shown in Fig. 3. The cylinder was placed 8 mm (0.31 in.) from the exit of the nozzle. The asymptotic bow shock angle indicates a Mach number of 1.53, but recall that the cylinder is within a region of expanding flow. Mach waves observed near the exit of the nozzle give an exit Mach number of about 1.35. The complex shock structure aft of the cylinder may in part be due to three-dimensional effects as well as impingement of the side expansion shear layers on the model mounting plate. Using the jump in light intensity as an indicator of density ratio across the shock, intensity ratios of about 1.2–1.3 were common. This is consistent with the density ratios expected for the Mach numbers tested here.

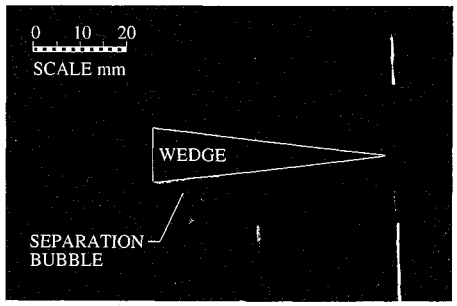

Fig. 4 Flow over a 5.8-deg half-angle wedge with Mach 1.5 nozzle.

Figure 4 shows the 5.8-deg wedge placed 2 mm (0.08 in.) from the exit of the Mach 1.5 nozzle. The shock induced boundary-layer separation occurs at the same location downstream of the nozzle exit as in Fig. 3. This is to be expected since the incident shock wave is produced by the overexpanded jet and is not a function of model position. Here the separation bubble is about 3 mm thick. This strong interaction suggest that the boundary layer on the wedge is laminar.

IV. Conclusion

A flow visualization method suitable for high-speed flows has been demonstrated. The laser light sheet combined with digital imaging provides a capability to resolve flow structure with low-light levels. The images obtained in this study clearly show the extent and location of shock waves as well as boundary-layer interactions. Natural condensation of water vapor was found to provide more than adequate light scattering particles for flow visualization. A flow tracer may need to be injected into flows where stagnation conditions are not conducive to natural condensation. The thermodynamic effect of condensation on the flow must be considered in determining the amount of injection so that local stagnation temperatures are not significantly altered. With appropriate seeding and illumination, the adaptation of the present scheme to an operating compressor rotor using a pulsed laser light source appears promising. Technical details are currently under study.

Acknowledgments

This work was sponsored by the Aero Propulsion and Power Directorate, Wright Laboratory, Wright–Patterson Air Force Base, Ohio, under Contract F33615-90-C-2086. The author gratefully acknowledges the assistance of David Bell in conducting the experiments described in this Note.

References

[1]Mueller, T. J., "Flow Visualization by Direct Injection," *Fluid Mechanics Measurements*, edited by R. J. Goldstein, Hemisphere, New York, 1983, pp. 307–375.

[2]Goddard, V. P., McLaughlin, J. A., and Brown, F. N. M., "Visual Supersonic Flow Patterns by Means of Smoke Lines," *Journal of Aerospace Sciences*, Vol. 26, No. 11, 1959, pp. 761, 762.

[3]McGregor, I., "The Vapour-Screen Method of Flow Visualization," *Journal of Fluid Mechanics*, Vol. 11, 1961, pp. 481–511.

[4]Campbell, J. F., Chambers, J. R., and Rumsey, C. L., "Observation of Airplane Flowfields by Natural Condensation Effects," *Journal of Aircraft*, Vol. 26, No. 7, 1989, pp. 593–604.

Errata

Simple Method of Supersonic Flow Visualization Using Watertable

A. K. Pal and B. Bose
Jadavpur University, Calcutta 700032, India

[AIAA Journal, 33(1), pp. 181–182 (1995)]

DURING production of this paper, two figures were switched. Their correct placement and captions are

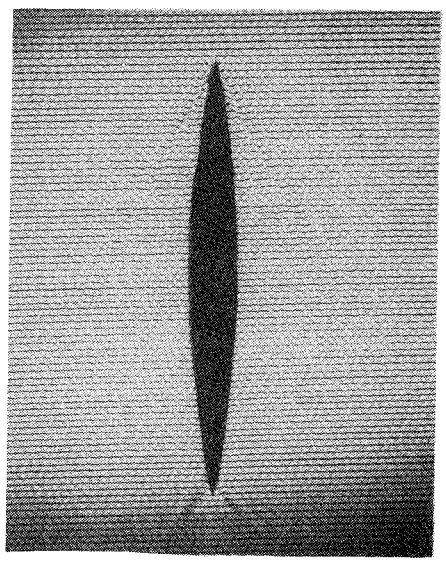

Fig. 2 Symmetric airfoil (maximum thickness 16 mm, chord length 144 mm) at Mach number 2.82.

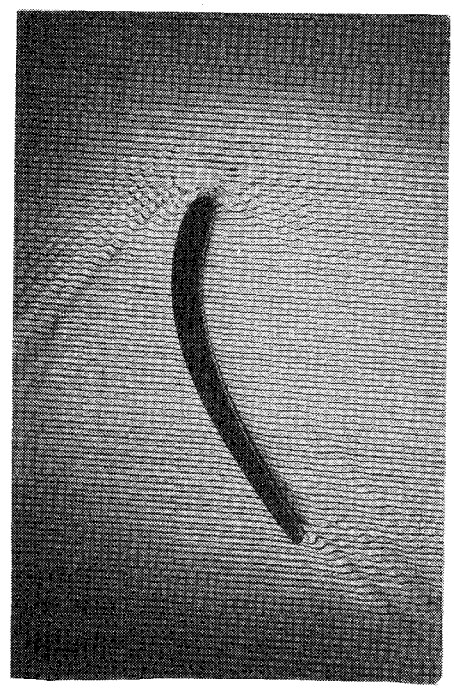

Fig. 3 Cambered airfoil at Mach number 1.86.

AIAA regrets this error.